Variability of the Intermediate Atlantic Water of the Arctic Ocean over the Last 100 Years

I. V. POLYAKOV,* G. V. ALEKSEEV,+ L. A. TIMOKHOV,+ U. S. BHATT,* R. L. COLONY,* H. L. SIMMONS,* D. WALSH,# J. E. WALSH,* AND V. F. ZAKHAROV+

*International Arctic Research Center, University of Alaska Fairbanks, Fairbanks, Alaska
+Arctic and Antarctic Research Institute, St. Petersburg, Russia
#Naval Research Laboratory, Stennis Space Center, Mississippi

(Manuscript received 12 March 2004, in final form 17 June 2004)

ABSTRACT

Recent observations show dramatic changes of the Arctic atmosphere–ice–ocean system, including a rapid warming in the intermediate Atlantic water of the Arctic Ocean. Here it is demonstrated through the analysis of a vast collection of previously unsynthesized observational data, that over the twentieth century Atlantic water variability was dominated by low-frequency oscillations (LFO) on time scales of 50–80 yr. Associated with this variability, the Atlantic water temperature record shows two warm periods in the 1930s–40s and in recent decades and two cold periods earlier in the century and in the 1960s–70s. Over recent decades, the data show a warming and salinification of the Atlantic layer accompanied by its shoaling and, probably, thinning. The estimate of the Atlantic water temperature variability shows a general warming trend; however, over the 100-yr record there are periods (including the recent decades) with short-term trends strongly amplified by multidecadal variations. Observational data provide evidence that Atlantic water temperature, Arctic surface air temperature, and ice extent and fast ice thickness in the Siberian marginal seas display coherent LFO. The hydrographic data used support a negative feedback mechanism through which changes of density act to moderate the inflow of Atlantic water to the Arctic Ocean, consistent with the decrease of positive Atlantic water temperature anomalies in the late 1990s. The sustained Atlantic water temperature and salinity anomalies in the Arctic Ocean are associated with hydrographic anomalies of the same sign in the Greenland–Norwegian Seas and of the opposite sign in the Labrador Sea. Finally, it is found that the Arctic air–sea–ice system and the North Atlantic sea surface temperature display coherent low-frequency fluctuations. Elucidating the mechanisms behind this relationship will be critical to an understanding of the complex nature of low-frequency variability found in the Arctic and in lower-latitude regions.

1. Introduction

Exchanges between the Arctic and North Atlantic Ocean have a profound influence on the circulation and thermodynamics of each basin (Aagaard and Carmack 1994). The Arctic Ocean is one of the major source regions for the surface waters of the subpolar seas in which weak stratification leads to deep convection, a key part of the global thermohaline circulation (Dickson et al. 2000). The warm and salty Atlantic water (AW) plays a special role in the thermal balance of the Arctic Ocean. It enters the Norwegian Sea through the Faeroe–Shetland Channel as the Norwegian Current. Part of this flow continues east on the Barents Sea shelf (see Fig. 1 for geographical notations), while another part, the West Spitsbergen Current, flows toward Spitsbergen. There it merges with colder and fresher Arctic surface water, sinks to intermediate levels, and flows into the Arctic Ocean. The Norwegian Current supplies the Arctic Ocean with AW, forming a warm (temperature $>$ 0°C) intermediate layer. Within the Arctic interior the subsurface AW circulation is strongly affected by bottom topography, flowing cyclonically along the basin margins (Rudels et al. 1994; Fig. 1).

Isolated from drifting ice by a fresh and cold surface layer, the intermediate AW carries vast quantities of heat. Maximum (2°–3°C) AW core temperatures (AWCTs) are found in the Nansen Basin, while in the Canadian Basin the AWCT does not exceed 0.4°–0.6°C (Treshnikov 1985). This AWCT decrease provides evidence that some fraction of AW heat is lost along the AW pathways. However, mechanisms of the AW ventilation are still very uncertain. For example, the substantial AWCT decrease along the Nansen Basin slope cannot be explained by a diapycnal diffusion. There are, however, some indications that AW heat may be lost above the upper slope of the Laptev Sea (Schauer et al. 1997; D. Walsh et al. 2004, unpublished manuscript).

Corresponding author address: Dr. I. V. Polyakov, International Arctic Research Center, University of Alaska Fairbanks, P.O. Box 757335, Fairbanks, AK 99775.
E-mail: igor@iarc.uaf.edu

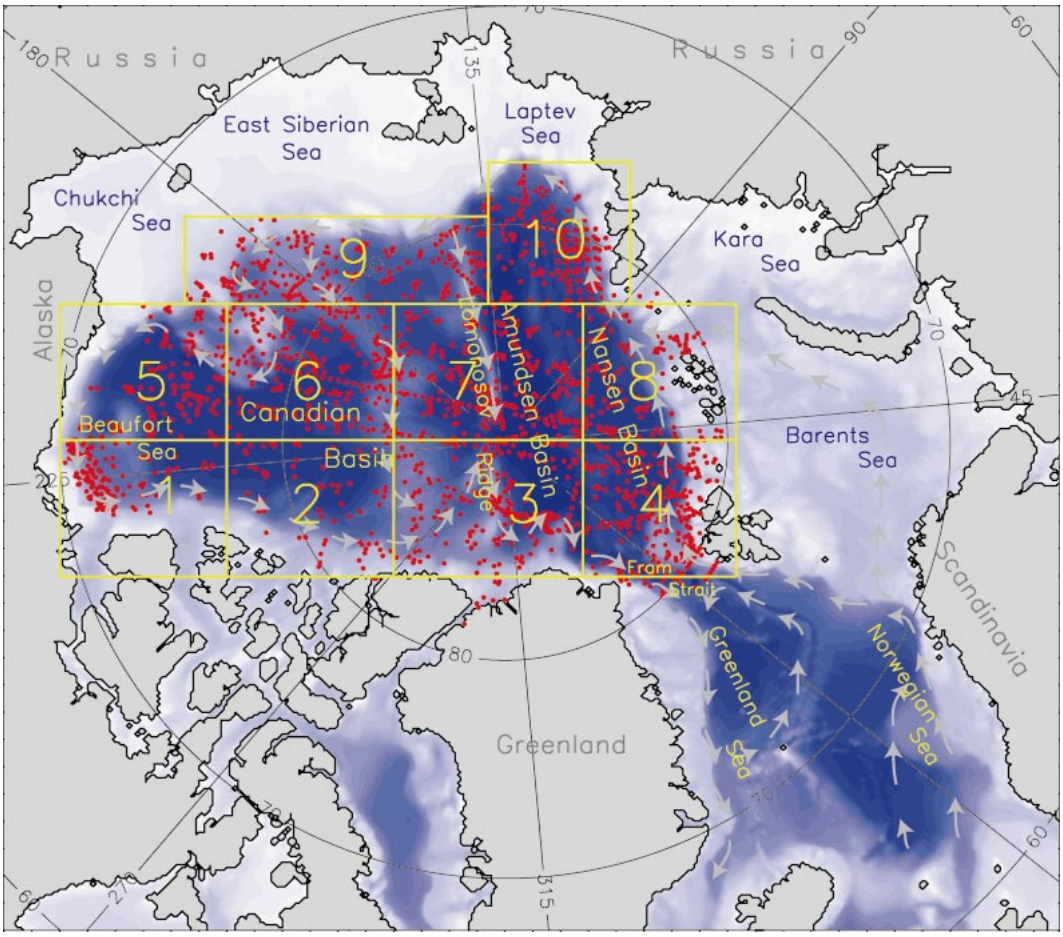

FIG. 1. Map of the Arctic Ocean. Locations of oceanographic stations used in this study are shown by red dots. Boxes delineate regions used in the analysis of the ocean temperature. The pathways of Atlantic water generally follow topographic contours keeping shallow regions on their right and are shown schematically by gray arrows.

Released into the upper ocean, this heat has the potential to melt substantial quantities of Arctic ice. Carmack et al. (1997) speculate that the strong lateral thermohaline interleaving may account for the decrease in AWCT.

Over the past several decades, the Arctic has undergone substantial changes (Serreze et al. 2000; Morison et al. 2000; Overland et al. 2004). Enhanced transport of warmer air from lower latitudes (Serreze et al. 1997) leads to increased arctic surface air temperature (SAT; Martin et al. 1997; Rigor et al. 2000) associated with decreased arctic sea level pressure (SLP), increased polar atmospheric cyclonicity (Walsh et al. 1996), and storminess (Zhang et al. 2004). Concurrent with these atmospheric changes are reductions in arctic ice extent (Johannessen et al. 1995; Maslanik et al. 1996; Cavalieri et al 2003; Vinje 2001) and a decrease of ice thickness (Rothrock et al. 1999; Tucker et al. 2001). Extreme amplification of the polar vortex in the late 1980s and early 1990s triggered significant changes in the upper Arctic Ocean. Steele and Boyd (1998) found a retreat of fresh surface waters and the loss of the cold halocline layer from the Eurasian Basin in the 1990s. In contrast, near-surface observations in the Canadian Basin in the 1990s showed strong freshening (McPhee et al. 1998).

The first evidence of strong warming in the Atlantic Water layer was found in the Nansen Basin in 1990 (Quadfasel et al. 1991). Positive AWCT anomalies of up to 1°C were carried along the continental margin into the Arctic Ocean interior (Carmack et al. 1995, 1997; Steele and Boyd 1998; Morison et al. 1998b, 2000; Swift et al. 1997; SCICEX 2004). Increased transport of water caused a displacement toward the Canadian Basin of the Pacific–Atlantic water boundary (Carmack et al. 1995; McLaughlin et al. 1996; Morison et al. 1998b). Yearlong mooring observations on the slope of the eastern Amundsen Basin in 1995–96 showed generally warmer AWCT, by about 1°C, compared with climatologies (Woodgate et al. 2001). Both observations (Woodgate et al. 2001) and modeling (Karcher et al. 2003) indicate a highly variable nature of the AW flow, with abrupt cooling/warming events that complicate the investigation of long-term variability in the AW.

It is quite possible that many of the recent changes described above can in part be attributed to large-am-

TABLE 1. Observations used in this study. Footnotes identify data sources.

Expedition (source)	Time	Region	Number of stations
Nanesn[a]	1893–96	Eurasian Basin	28
Various expeditions[b]	1899–1959	Arctic Ocean	515
bsvar[c]	1950–87	Beaufort Sea	1541
sever25–31[b]	1973–79	Arctic Ocean	1034
Melling[c]	1979–94	Canada Basin	424
lorex[c]	1979	Arctic Ocean	2
ymer[c]	1980	Fram Strait	20
eubex[c]	1981	Eurasian Basin	37
cesar[c]	1983	Arctic Ocean	44
polarstar84[a]	1984	Eurasian Basin	70
polygon[b]	1984, 1985, and 1989	Nansen Basin	195
aiwex[a]	1985	Arctic Ocean	7
polarstar87[a]	1987	Eurasian Basin	59
nogap[c]	1987–93	Beaufort Sea	53
ice89[c]	1989	Canadian Basin	6
oden91[a]	1991	Eurasian Basin	51
scicex[a]	1993 and 1997–98	Arctic Ocean	278
aos94[a]	1994	Arctic Ocean	110
sheba[d]	1997–98	Canadian Basin	40
npeo[a]	2000–02	North Pole area	27
nabos02[e]	2002	Eurasian Basin	22

[a] National Snow and Ice Data Center (available online at http://nsidc.org).
[b] Arctic and Antarctic Research Institute, St. Petersburg, Russia.
[c] Environmental Working Group (1997).
[d] SHEBA (available online at http://sheba.apl.washington.edu).
[e] International Arctic Research Center.

plitude multidecadal fluctuations with a time scale of 50–80 yr. This high-latitude low-frequency variability [dubbed ''LFO'' (low-frequency oscillation), Polyakov and Johnson (2000)] is evident in various climatically important parameters of the Arctic air–sea–ice system (Mysak et al. 1990; Yi et al. 1999; Venegas and Mysak 2000; Polyakov et al. 2002, 2003a,b) as well as in proxy records (Delworth and Mann 2000). Understanding the mechanisms behind this variability is not trivial due to its evolving spectrum and changing relationship with large-scale climate parameters like the North Atlantic Oscillation (NAO). However, spectral analysis of the NAO index time series from 1886 to 1994 shows a significant portion of energy concentrated at about 0.02 (cycle/year), a period of approximately 50 yr (Yi et al. 1999, see their Fig. 9b). In contrast to the warming of the 1990s, the 1930s warm period in the Arctic did not coincide with a positive phase of the NAO, which has led Bengtsson et al. (2004) to argue, using observations and model results, that the early twentieth-century warming is associated with local Arctic air–sea–ice interactions.

Schlesinger and Ramankutty (1994) have documented multidecadal variability in Northern Hemispheric surface air temperatures that is particularly strong in the North Atlantic sector. This low-frequency oscillation (LFO) is evident in various instrumental records of the Northern Hemisphere [see Delworth and Mann (2000) for numerous references therein]. For example, Minobe (1997) analyzed SLP over the central North Pacific Ocean, SAT in western North America, sea surface temperature (SST) in the eastern North Pacific, Indian Ocean–Maritime Continent region, and in Japan, and reconstructed SAT from tree rings in North America. Minobe found variability with approximate time scales of 70 yr. Surface marine observations in the North Atlantic display distinct basinwide patterns of multidecadal SST variability (Kushnir 1994). According to the analysis of a long-term integration of the Geophysical Fluid Dynamics Laboratory coupled atmosphere–ocean model, this variability is related to fluctuations in the thermohaline circulation in the North Atlantic, particularly in SST (Delworth and Mann 2000). The Atlantic Multidecadal Oscillation, identified in sea surface temperatures (Enfield et al. 2001), is associated with hydrological anomalies over North America, where an anomalously warm Atlantic is connected with precipitation deficits in the Midwest. It is yet to be understood how the Arctic multidecadal fluctuations fit into the global multidecadal variability and what the forcing mechanisms are. Here we demonstrate, through the analysis of a vast collection of previously unsynthesized observational data, that the AW variability exhibits a LFO-like pattern with prolonged positive and negative phases of the AW anomalies. This identifies a piece of the puzzle of how high-latitude variability is connected to the lower latitudes.

2. Data and methods

The data used in this study consolidates several datasets (Table 1). Measurements made by Nansen (1902)

during his famous drift on board *Fram* began the era of deep-sea observation in the Arctic Ocean. Occasional ship-based observations near Fram Strait occurred starting in the beginning of the twentieth century. Systematic oceanographic observations began only in the 1930s–40s, when the Russians started a monitoring program consisting of manned ice-drift stations and winter aircraft surveys complemented by ship-based studies during summer. In 1955–56 the first Russian basin-scale aircraft surveys were conducted. A few observations are available starting in the 1960s, but the 1970s was an exceptional period in the history of high-latitude exploration, with seven Russian winter aircraft surveys (1973–79) and 1034 oceanographic stations during this period. This information comprised the bulk of the data used to construct the atlases of the Arctic Ocean by Gorshkov (1980), Treshnikov (1985), and the Environmental Working Group (1997). Most measurements during the 1980s were made within limited, local areas. In the 1990s, the intensive use of icebreakers and submarines opened a new phase in the history of Arctic observation. Vast areas of the Arctic Ocean, previously limited to ship-based sampling in light ice conditions, were now within reach of these powerful scientific observational platforms. Data from only a few oceanographic casts carried out in the 2000s are available. The temporal distribution of measurements used in this study is shown at the bottom of Fig. 2 (top).

Most historical (prior to the 1980s) observations used Nansen bottles to take water samples and measure temperatures at standard levels. The accuracy of temperature and salinity measurements is estimated to be 0.01°C and 0.02 psu, respectively (Environmental Working Group 1997). While having rather coarse vertical resolution, the data provide good horizontal coverage, and the multiyear coverage makes the data an invaluable resource for use in understanding interannual variations of the water mass structure within the Arctic Ocean. Polyakov et al. (2003c) showed that the coarse vertical resolution of the historical data in the vicinity of the AW core allows the AWCT to be computed quite accurately, but the precise depth of the temperature maximum cannot be accurately deduced from the data. In recent years CTD measurements were obtained, which have accuracies at least an order of magnitude greater than the bottle measurements.

Because maximum AWCT variability is found in the Eurasian Basin, with variability decreasing toward the Beaufort Sea (Polyakov et al. 2003c), a direct comparison of AWCT fluctuations from different Arctic Ocean regions is problematic. However, we can obtain comparable regional quantities by reducing AWCTs from different regions to their anomalies and normalizing these anomalies by their respective regional standard deviations. This approach was first proposed by G. Alekseev and has been used for analysis of the AWCT (G. Alekseev et al. 2003, unpublished manuscript). Alekseev et al. were first to show the existence of multidecadal mode of variability in the AWCT data. Because the latter study was based on an analysis of only 187 stations within eight local Arctic regions, the statistical estimates were not well constrained. In our study, the Arctic Ocean is divided into ten boxes (regions) of approximately equal areas (Fig. 1). Individual (snapshot) measurements over the ten regions were averaged within a given year and region to produce ten regional time series of composite AWCT. The length of the regional composite records is shown in Table 2. Based on these composite values, regional means ($\overline{T}_{\text{reg}}$) and standard deviations (σ_{reg}) were calculated (Table 2). Each regional composite value was then reduced to an anomaly relative to its regional mean $\overline{T}_{\text{reg}}$ and normalized by its regional σ_{reg}. These normalized regional AWCT anomalies are shown in Fig. 2 by gray numerals that correspond to the region they represent (i.e., ''1'' corresponds to values for Region 1, etc.). The red curve represents normalized regional AWCT anomalies averaged over these ten regions. Sensitivity to our regional statistical estimates of AWCT mean and variations to region size, location, and averaging procedure within each box is discussed in the appendix.

3. Long-term Atlantic water core temperature variability

a. Long-term variability and trends

The normalized AWCT anomalies (Fig. 2, red) show two distinct warm periods from the late 1920s to 1950s and in the late 1980s–90s and two cold periods, one at the beginning of the record (until the 1920s) and another in the 1960s–70s. The differences between 15-yr averages at the LFO peaks (horizontal lines in Fig. 2, top) emphasize different thermal conditions during warm and cold periods. The same periods stand out for the Arctic SAT [green line in Fig. 2, middle, see also Polyakov et al. (2003a)], ice extent and fast-ice thickness from the Arctic Siberian seas [blue line in Fig. 2, middle, see also Polyakov et al. (2003b)], ocean salinity in the upper 50 m of the Barents Sea (Polyakov and Johnson 2000), as well as other climatically important high-latitude parameters. These AWCT changes compare favorably with the warming trend found in 1978–93 based on a record of the mean water temperature between 50 to 200 m in the West Spitsbergen Current south of Svalbard (Blindheim et al. 2000). The above periods were attributed to the positive/negative phases of low-frequency oscillation (LFO) with higher/lower maritime Arctic SAT and atmospheric vorticity, lower/higher SLP, and reduced/increased ice concentration and landfast ice thickness in the Arctic marginal seas (Polyakov and Johnson 2000). The similarity between the normalized AWCT anomalies (red), composite Arctic SAT (green), and fast ice thickness (blue) is particularly striking, with concurrent warm and cold phases that correspond to decreases and increases of fast ice thickness (Fig. 2, mid-

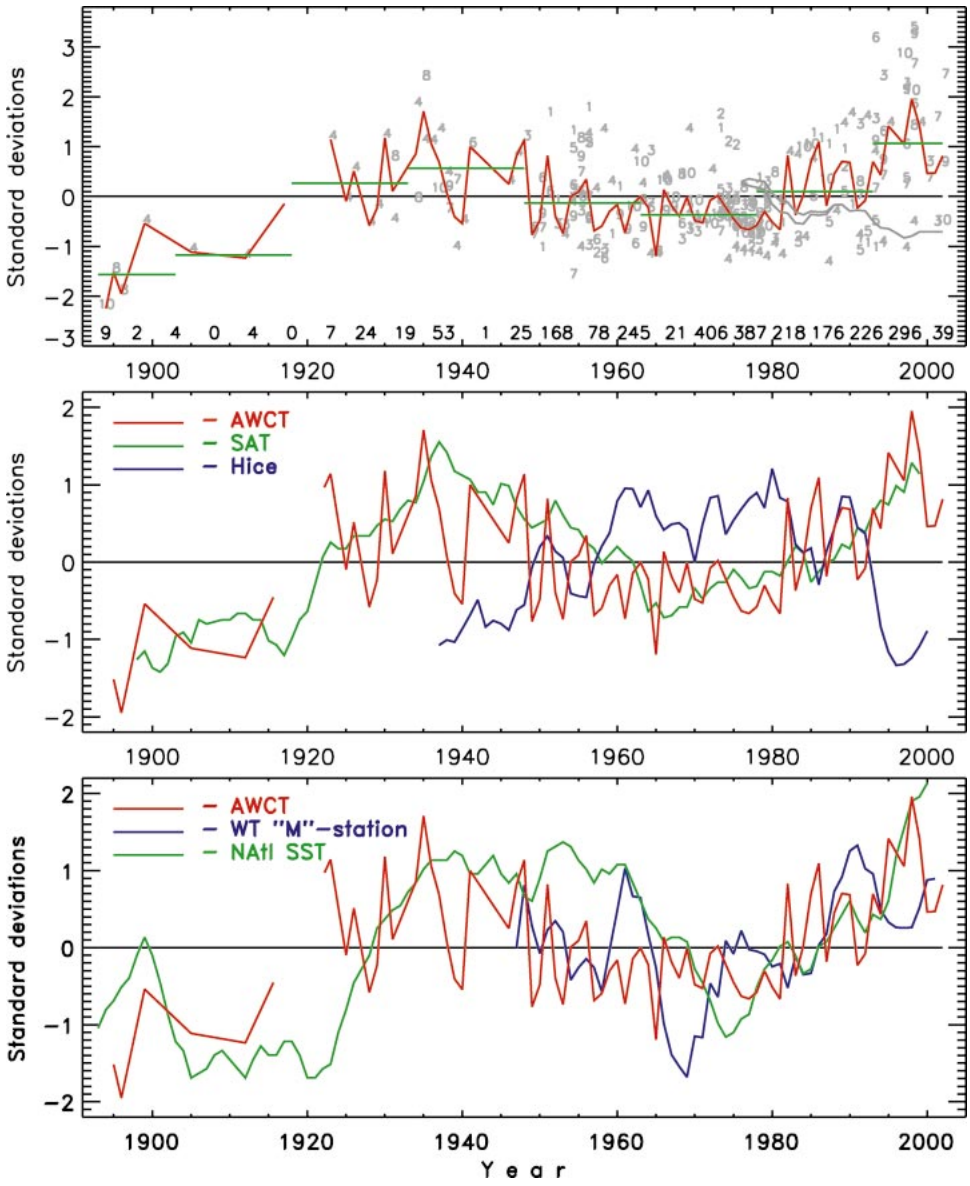

FIG. 2. Long-term variability of the Atlantic water temperature. (top) Gray numbers represent normalized Atlantic water core temperature (AWCT) anomalies for the 10 regions outlined in Fig. 1. Averaged annual values of the normalized AWCT anomalies are shown by the red line (dashed segments represent gaps in the record). Green horizontal lines show 15-yr means. Two highly correlated gray lines show the AW layer thinning (solid) and shoaling (reduction of the upper-boundary depth; dashed) in the late 1970s–90s. Numbers at the bottom of the panel denote the 5-yr-averaged number of stations used in the data analysis. (middle) For comparison, in addition to the normalized AWCT anomalies (red), a composite time series of the normalized 6-yr running mean Arctic SAT anomalies (Polyakov et al. 2003a) (green) and normalized time series of 6-yr running mean anomalies of fast ice thickness at station Sterlegova (Kara Sea, blue) are shown. (bottom) Linkage between processes in the Arctic and North Atlantic. The AWCT (red), normalized 6-yr running mean 10-m water temperature anomalies from ocean weather station Mike at 66°N, 2°E (Norwegian Sea, blue), and normalized North Atlantic SST anomalies from the region limited by 0°–90°N, 290°–30°E (green) are shown.

dle). There are, however, some important differences: while the Arctic SAT reaches its warmest temperatures in the 1930s–early 1940s, the AWCT displays slightly higher temperatures in recent decades. It is possible that undersampling in the 1930s–40s may impact that part of the AWCT record.

A background warming trend (evaluated by the least squares method) for 1893–2002 of about 0.13 ± 0.04

TABLE 2. AWCT regional means ($\overline{T}_{reg}$), standard deviations (σ_{reg}), and the length N (number of years with data) used to calculated these statistics.

Region	1	2	3	4	5	6	7	8	9	10
N	27	12	26	59	18	24	23	19	23	24
$\overline{T}_{reg}$	0.44	0.42	0.62	3.72	0.49	0.57	0.91	1.67	0.73	1.31
σ_{reg}	0.03	0.03	0.20	1.72	0.06	0.12	0.16	0.43	0.24	0.32

standard deviation (σ) of the annual mean AWCT per decade is also apparent from the AWCT record (Fig. 2). Analyzing Arctic SAT trends, it was shown that the trends are strongly modulated by pronounced multidecadal variability (Polyakov et al. 2002), which may in some cases overwhelm long-term trends. It was argued that multidecadal variability had little net effect on computed trends during the twentieth century since positive and negative LFO phases fortuitously cancel each other. Extending this argument to the AWCT, we calculate the contribution of multidecadal fluctuations to AWCT change in recent decades. The difference between decadal means for the 1970s and 1990s is about $1.17 \pm 0.21\sigma$, approximately 20% of which is apparently due to the long-term trend, whereas 80% of the observed recent AW warming may be attributed to the multidecadal variability. Caution is required in the analysis of regional trends due to a dearth of observations, especially in the early parts of the record. Because of the above assumptions and a wide range of uncertainties, our estimates must be viewed as approximate, qualitative measures of the AWCT trends and variations.

b. Atlantic water during positive and negative LFO phases

It is fortunate that the densest data coverage falls in the 1970s and 1990s, corresponding to a negative and positive phase of the multidecadal temperature variability, thus allowing a detailed analysis of differences between these two LFO phases. High 1980–90 values of the NAO index, characterized by a north–south oriented dipole in sea level pressure over the Atlantic (Hurrell 1995), drove warmer water from the North Atlantic into the Norwegian Sea and farther into the Arctic Ocean (Swift et al. 1997; Dickson et al. 2000). This likely enhanced the inflow of warmer water, resulting in higher temperatures along the AW pathways (Fig. 3) (see also Swift et al. 1997; Grotefendt et al. 1998; Morison et al. 1998b; Steele and Boyd 1998). For example, the position of the 0.75°C isotherm in the 1990s was shifted more than 1000 km farther east along the Siberian continental slope compared with the 1970s (Fig. 3). There is evidence of relatively uniform AW in the Nansen Basin, with a front along the Nansen–Gakkel Ridge in the 1990s (Swift et al. 1997; Steele and Boyd 1998). Note the surprisingly high speed with which the positive anomaly propagated into the Arctic Ocean interior where within one decade (1990s) vast areas of the polar basin were filled with anomalously warm water (Fig. 3). This fact seems to contradict isotope-based renewal times of the order of 1–2 decades suggested by Smethie et al. (2000). The same discrepancy between estimates deduced from current measurements and chlorofuorocarbon (CFC) age calculation was noticed by Woodgate et al. (2001, see p. 1774). There was less warming in the 1990s in the eastern part of the Canadian Basin (Fig. 3), as was also shown by Pawlowicz and Farmer (1997). Associated with the recent warming was AW salinification; in particular, the basinwide averaged salinity within the 200–800-m layer increased from 34.80 psu in the 1970s to 34.84 psu in the 1990s.

Averaged over the Arctic Ocean, AW heat content (not shown) was larger by about 4.3×10^8 J m^{-2} in the 1990s compared with the 1970s, which constitutes approximately 9% of the total AW heat content. Approximately 80% (or $\sim 3.4 \times 10^8$ J m^{-2}) of this heat may be arguably attributed to multidecadal fluctuations if arguments similar to those used to separate low-frequency AWCT variability from long-term trends are applied. This component of AW heat content appears to fluctuate with a half-period of 25–30 yr and, when expressed as an effective vertical flux, represents an oscillatory flux with an amplitude of 0.4–0.6 W m^{-2}. Estimates of upward heat flux from the AW yield values from 1.3 W m^{-2} [analytical model (Rudels et al. 1996)] to 2.1 W m^{-2} [one-dimensional mixed-layer model (Steele and Boyd 1998)], 3–4 W m^{-2} [parameterization for the bulk heat transfer coefficient from the mixed layer temperature (Krishfield and Perovich 2004, manuscript submitted to *J. Geophys. Res.*)], 4–6 W m^{-2} [heat budget estimates for the eastern Nansen Basin (D. Walsh et al. 2004, unpublished manuscript)], and as large as 15–30 W m^{-2} for the Eurasian Basin interior and 150–160 W m^{-2} for its shelf and slope areas [estimates based on parameterizations of vertical mixing in the oceans, Dewey et al. (1999)]. Using observed melting rates and temperature profiles within ice, McPhee and Untersteiner (1982) estimated an oceanic heat flux of less than 2 W m^{-2} to the ice in the region northwest of Spitzbergen, placing an upper limit on thermocline heat fluxes in this area. Thus the LFO-associated component of heat flux may constitute between 10% and 50% of current heat flux estimates [excluding somewhat extreme estimates by Dewey et al. (1999)]. This flux of 0.4–0.6 W m^{-2} could cause 0.8–1.0 m loss in ice thickness over the last 20 years or approximately the amount seen in recent decades (Rothrock et al. 1999). Note that these estimates are based on the severe assumption that all heat is mixed upward from the AW

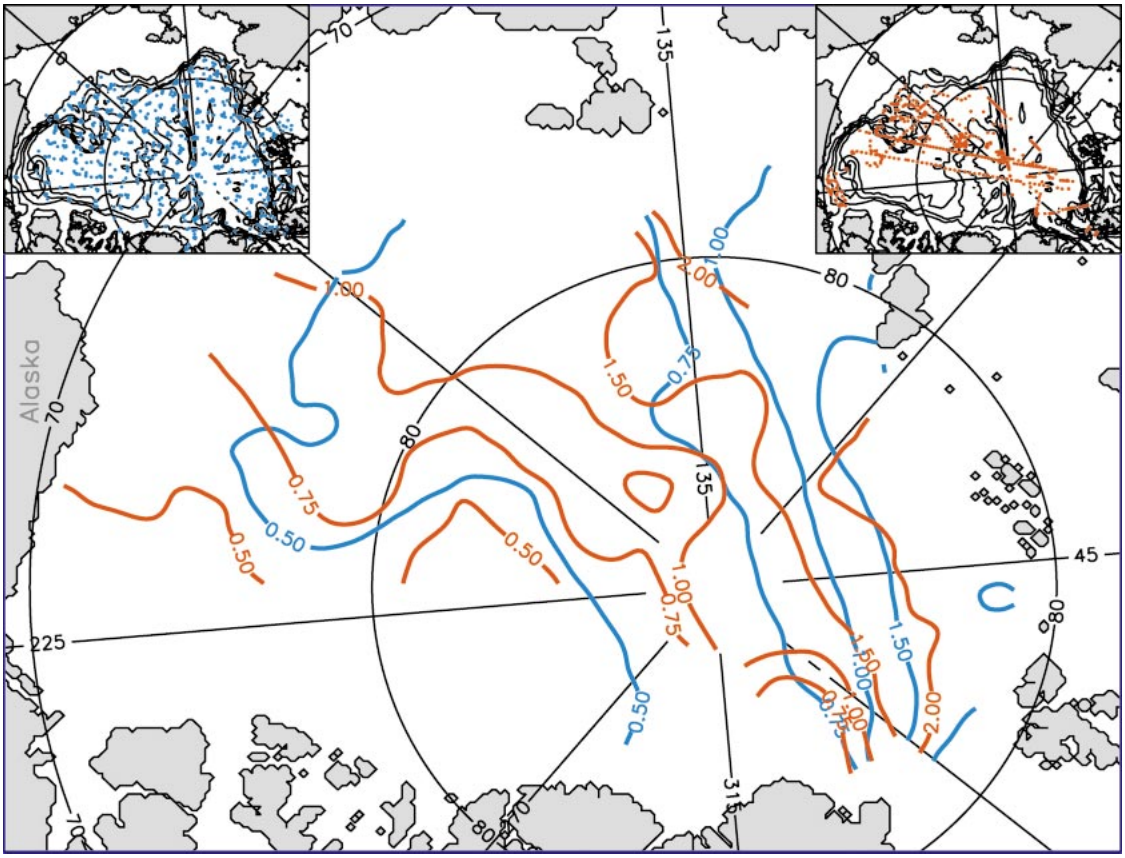

FIG. 3. Spatial distributions of the AW temperature anomalies (°C) averaged over the positive (1990s, red) and negative (1970s, blue) phases of the multidecadal variability (some smoothing based on the Laplacian operator is applied). Data coverage for each decade is shown in the panels inserted at the top corners with blue (red) dots representing the 1970s (1990s). Warm AW in the 1990s has spread farther in the basin interior along the Siberian continental slope than in the 1970s.

and through the near-surface freshwater cap to the surface. There is evidence that suggests upward fluxes occur preferentially in near-slope locations where especially strong convective mixing occurs (Steele and Morison 1993; D. Walsh et al. 2004, unpublished manuscript). Modeling results (e.g., Häkkinen and Mellor 1992) also suggest strong spatial variations of the oceanic heat flux. Thus, we may expect greater localized heat fluxes associated with anomalously high AW heat content during positive LFO phases than during cooler negative phases.

Recent changes in the Arctic atmosphere are consistent with a dipolelike scheme of alternating Arctic atmospheric circulation regimes with weakened/strengthened anticyclonic Beaufort gyre and intensified/suppressed cyclonic circulation in the eastern Arctic [Gudkovich (1961); see our schematic Fig. 4, which is updated and adapted from Proshutinsky and Johnson (1997)]. These changes in atmospheric circulation have a profound effect on the Arctic ice and oceanic conditions. For example, Proshutinsky and Johnson (1997) found periods of intensified cyclonic/anticyclonic ice drift to be associated with decadal cyclonic/anticyclonic atmospheric circulation regimes. Walsh et al. (1996) argued that cyclonic winds cause divergent ice drift resulting in overall thinner ice, while anticyclonic winds produce convergent ice motion and generally thicker ice. It has been hypothesized that cyclonic winds and divergence of ice drift and surface currents elevate the upper AW boundary (Proshutinsky and Johnson 1997). Our data confirms that the divergence of prevailing cyclonic winds and surface circulation in the late 1980s–90s resulted in shoaling of the AW upper boundary by about 75 m with the center in the Makarov Basin (see gray dashed line in Fig. 2). Steele and Boyd (1998) previously reported that the AW layer shoaled by about 40 m within the Amundsen Basin. Shoaling of the AW core was also reported by Morison et al. (1998a).

Carmack et al. (1997) and Swift et al. (1997) provided the first observational evidence that the AW core was also elevated in the 1990s compared with the 1970s. Our data confirm that the AW core was lifted by approximately 150 m in recent decades, providing the spatial pattern of this anomaly (Fig. 5, left column). The location of this domelike anomaly is in close proximity to the location of zonally symmetric cells of SLP dif-

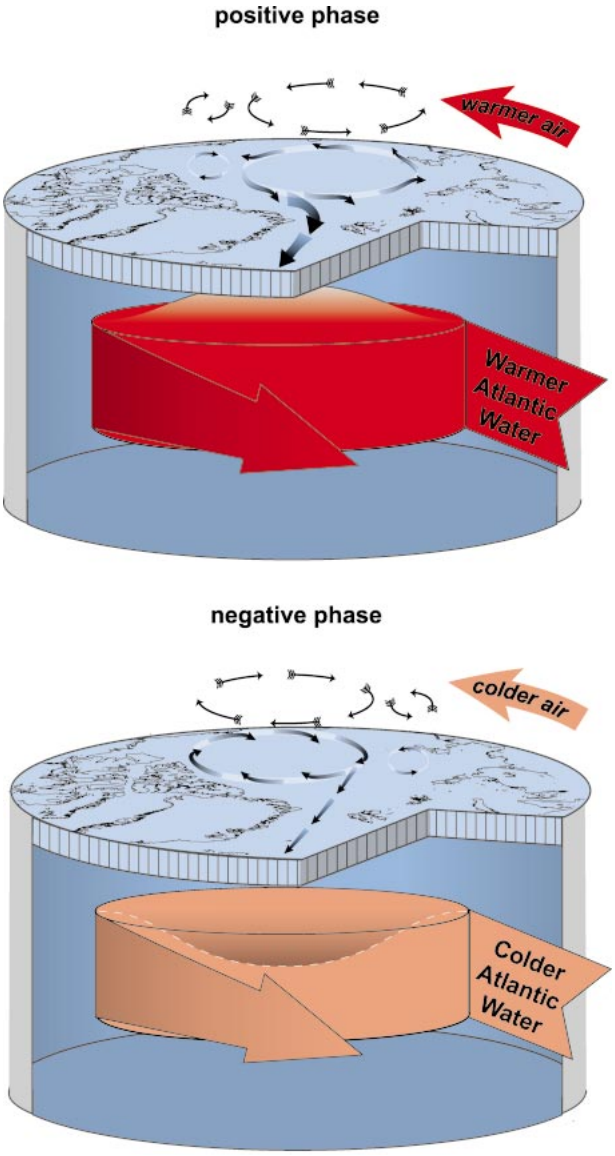

FIG. 4. A schematic showing atmospheric and oceanic circulation during the two phases of multidecadal variability (LFO) in the Arctic. During the positive phase, there is an increase of transport of warmer air and water from the North Atlantic into the Arctic. The anticyclonic Beaufort gyre is weakened/strengthened, and cyclonic circulation in the eastern Arctic is intensified/suppressed during positive/negative LFO phase. During the positive LFO phase, there is excess ice and freshwater transport through Fram Strait from the Arctic, suppressing deep-water convection in the Greenland Sea. Increased cyclonicity under the positive phase of multidecadal variability causes divergence of ice drift and surface circulation, leading to doming of the AW. The well-developed Arctic high, evident during negative LFO phases, results in intensified anticyclonic ice drift and surface circulation, convergence of surface currents, and a depression in the AW.

ference between the two LFO phases (Polyakov and Johnson 2000), which bear a strong resemblance to the multidecadal SLP pattern (Johnson et al. 1999) and the Arctic Oscillation pattern (Thompson and Wallace 1998). Surprisingly, our data suggest that, on the basin scale, the AW layer does not thicken during the positive LFO phase, in conjunction with probably enhanced AW inflow. In fact, the data suggest thinning of the AW layer (the gray solid line in Fig. 2), which is highly correlated in time with the AW layer shoaling. Note, however, that there are numerous local (mostly at the deep basin margins) deviations from this general tendency. Also, the precise depth of the AW lower boundary and, therefore, its thickness cannot be accurately determined from the historical data due to the coarse resolution (100–150 m) of measurements in the deeper AW layer.

c. Possible regulatory mechanism of the Atlantic water inflow

The sustained warming tendency in the AW layer stopped in the late 1990s (Boyd et al. 2002; Morison et al. 2002), consistent with a weakening of the positive phase of the multidecadal component of the NAO index (Hurrel 2003). The differences in the spatial distributions of the integrated (0–800 m) density in the 1970s and 1990s (Fig. 5, right column) may shed light on one of the reasons why by the end of the 1990s the positive temperature anomaly had decreased in the Arctic Ocean. During the 1970s, the density minimum is centered in the Canada Basin and is associated with the Beaufort gyre (Fig. 5, top). During the 1990s, this minimum is displaced farther toward the Canadian coast (Fig. 5, middle). Thus, starting in the 1980s, increased inflow of salty North Atlantic water into the Arctic Ocean (see our Fig. 2) resulted in overall denser water in the upper 800 m (roughly the depth of the AW bottom boundary). The spatial pattern of this anomaly resembles that of the AWCT depth and has a maximum in the central Arctic Ocean (cf. Fig. 5, bottom left and right).

This spatial distribution of the density anomaly causes a water particle to move from areas with higher density (or pressure) to lower density (i.e., from the center of the basin toward its periphery) with a deflection to the right due to the earth's rotation (i.e., Coriolis force) suggested by a simple geostrophic balance. Note that in this balance we take into account vertically integrated density gradients only and thus neglect another effect of horizontal density inhomogeneties, which is density-induced sea level gradients. In general, these two parts of the density-dependent force work against each other. A modeling study showed that the sea level gradients prevail in the upper Arctic Ocean, driving circulation anticyclonically in a way similar to wind-induced surface circulation (Polyakov 1996). In the deeper layers of the Arctic Ocean, including the Atlantic water layer, density gradients are the major driving force moving water along the deep basin margins cyclonically. Since our goal here is to get a rough qualitative estimate of how density anomalies may possibly impact the AW circulation, our analysis of a simple balance of forces should be sufficient.

The resulting circulation tendency due to this balance

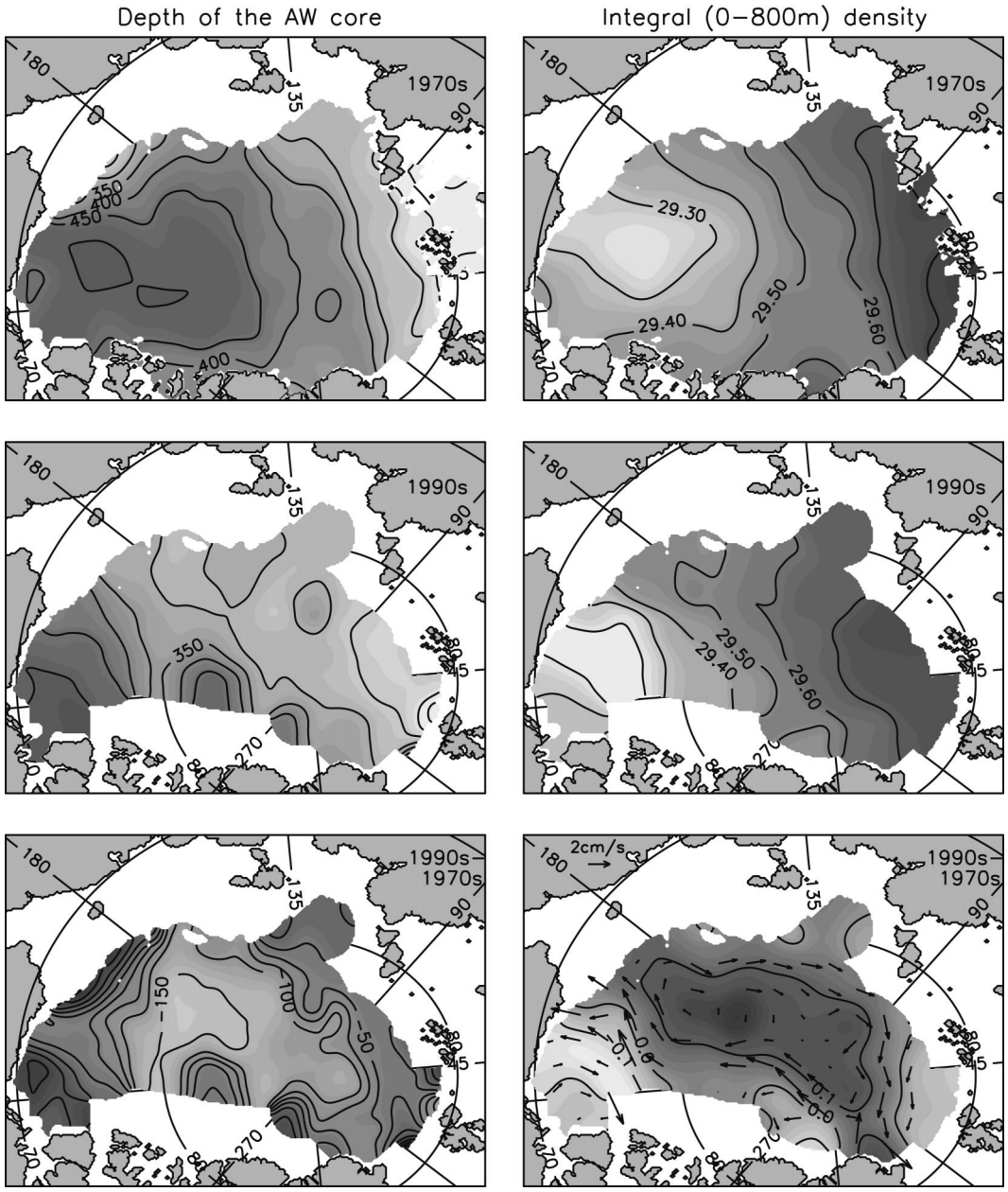

FIG. 5. (left) The depth of the AWCT and (right) the integrated 0–800-m density averaged over (top) the 1970s, (center) 1990s, and (bottom) their difference. Note that some smoothing based on the Laplacian operator is applied. Starting from the 1970s, the increased inflow of salty dense North Atlantic water induced positive density anomalies in the central Arctic Ocean. These anomalies suggest a geostrophic anomaly current (arrows), which acts to reduce inflow into the Arctic (i.e., negative feedback).

of density gradients and the Coriolis force is shown by arrows in Fig. 5 (lower right). It suggests that the density structure at the end of the 1990s acted to partially offset the inflow of Atlantic water into the Arctic Ocean. This negative feedback highlights the complex coupled nature of air–sea–ice interactions at high latitudes. In addition, this suggests that an internal Arctic mechanism plays an active role in high-latitude multidecadal variability, whether or not the fluctuations have a North Atlantic source.

d. Links between variability of the Atlantic water with processes in lower latitudes

Our data provide evidence that the AW variability is positively correlated with the hydrographic changes in

the Greenland and Norwegian Seas. Much of the variability in the AWCT is advected from upstream locations in the Norwegian Sea, as can be seen in a comparison of the AWCT (Fig. 2b, red) and the water temperature from the upper Norwegian Sea (blue, site of Ocean Weather Station Mike at 66°N, 2°E). Both AW and the upper Norwegian Sea display coherent fluctuations, with warmer water in the late 1940s–50s and 1980s–90s (positive LFO phases) and colder water in the 1960s–70s (negative LFO phase). Earlier studies suggest the importance of the Arctic Ocean for the deep hydrographic regime in the Greenland and Norwegian Seas (Aagaard et al. 1991). In recent decades, intermediate and deep waters of the Greenland and Norwegian Seas warmed and became more saline (Østerhus and Gammelsrød 1999; Bønisch et al. 1997; Dickson et al. 2000). It has been suggested that the warming and salinification were caused (among several reasons) by an enhanced exchange with the Arctic Ocean (Østerhus and Gammelsrød 1999), and the warmer and saltier AW found in the 1990s provides further support for this hypothesis.

Over the last 50 years Labrador Sea records show freshening and cooling (see, e.g., Fig. 1 of Dickson et al. 2002). These Labrador Sea changes have a maximum at a depth of 2000–3000 m but may be traced to shallower depths. The timing of these sustained anomalies of the deep Labrador Sea hydrography corresponds well to time intervals of anomalies of opposite sign found in the Atlantic water of the Arctic Ocean, and in the Greenland and Norwegian Seas. There is also evidence that convective activity in the Labrador and Greenland Seas is negatively correlated (Lazier 1980; Meincke et al. 1992; Dickson et al. 1996). Spread by deep circulation, these anomalies of opposite sign affect the water mass properties throughout the respective basins over a considerable range of depths (Østerhus and Gammelsrød 1999; Dickson et al. 2002).

In the broader view, we expect a coupling of low-frequency changes in the Arctic hydrography with those at lower latitudes on larger spatial scales. Indeed, Fig. 2 (bottom) shows a remarkable resemblance between time series of the AWCT (red) and North Atlantic SST (green) where Kaplan et al. (1998) data over the region 0°–90°N, 290°–30°E are used. Since the Arctic SAT, ice extent and fast ice thickness, and temperature of the intermediate Atlantic water of the Arctic Ocean display coherent low-frequency variations, we may expand this conclusion for the entire Arctic climate system. This resemblance suggests a strong coupling between the Arctic low-frequency oscillation and the Atlantic multidecadal oscillation, identified in sea surface temperatures (Enfield et al. 2001). Elucidating the mechanisms behind this relationship will be critical to our understanding of the complex nature of low-frequency variability found in the Arctic and at lower latitudes.

4. Conclusions

We examine long-term variability of the Atlantic water using high-latitude hydrographic measurements starting in the late nineteenth century. Despite gaps in the early parts of the record, our analysis provides evidence that AW variability is dominated by multidecadal fluctuations with a time scale of 50–80 yr (LFO). The resemblance between variability of the AW and other key climatic parameters such as air temperature and pressure (Polyakov et al. 2003a), ice extent and thickness (Polyakov et al. 2003b), sea level (Dvorkin et al. 2000), and Barents Sea salinity (Polyakov and Johnson 2000) is striking, suggesting a close connection between large-scale atmospheric circulation and Arctic ice and oceanic conditions. In addition to documenting the variability we would like to determine the extent to which observed fluctuations in AW structure and properties represent a ''static'' thermodynamic response and to what extent they are a dynamical response to winds driving the circulation. Clearly, the observed shoaling of the AW layer in the 1990s is heavily influenced by the dynamics, while temperature, salinity, and heat content fluctuations may be either dynamically or thermodynamically controlled. While discerning the detailed causes of the observed variability will require further investigation of observational and modeling data, our analysis suggests a possible negative feedback mechanism through which changes in density act to moderate the inflow of Atlantic water to the Arctic Ocean, and hence a potential local source for fluctuations in AW inflow. This negative feedback may in part explain the decrease in warm Atlantic water temperature anomalies evident in the late 1990s. Sustained concerted phases of warming/salinification and cooling/freshening in the Arctic Ocean and Greenland and Norwegian Seas, and the opposition of the variability in these basins and the Labrador Sea, are likely due to air–sea interaction on larger spatial scales. Indeed, the striking resemblance between the variability of the North Atlantic SST and AWCT supports a possible linkage of low-frequency variations occuring in the Arctic and North Atlantic. The coordinated set of changes in the Arctic air–sea–ice system and the North Atlantic SSTs emphasizes the possible importance of high-latitude regions to global climate since evidently ''a means exists of transferring the 'signal' of high-latitude climate change to the deep and abyssal headwaters of the global thermocline circulation'' (Dickson et al. 2002).

Acknowledgments. We thank J. Moss and C. Swingley for help in preparation of the manuscript. We also thank T. Delworth, M. Steele, N. Untersteiner, and T. Vinje for useful discussions, and L. Bulatov, P. Golovin, and V. Karpii for preparation of data. The manuscript improved from the insightful comments of the two anonymous reviewers. This research is a part of the ongoing NSF-funded IARC Program, Nansen and Amundsen Ba-

sins Observational System (NABOS). We thank the Frontier Research System for Global Change and Russian Fund of Fundamental Research for financial support.

APPENDIX

Error Estimates

Note a certain level of ''noise'' in the AWCT data—the scatter is partially due to real noise in the observational data, especially in regions where standard deviations are not much higher than the accuracy of observations, or in earlier parts of the record (Regions 1 and 2; see Table 2, Fig. 2). However, we believe this is also due to difficulties in choosing regions with spatially similar (homogeneous) properties. For example, in the 1990s when the data quality improved, estimates for the Fram Strait region (Region 4) still show some intraregion scatter, with both positive and negative anomalies. This dynamically rich region where the warm West Spitsbergen Current interacts with the cold East Greenland Current is characterized by a high level of variability (Polyakov et al. 2003c). Despite the relatively high intraregion variability, spatially and temporally averaged estimates provide a meaningful and valuable measure of AWCT trends and long-term variability.

Analysis of the sensitivity of our regional statistical estimates of $\overline{T}_{\text{reg}}$ and σ_{reg} to region size, location, and averaging procedure within each box demonstrates the robustness of these estimates. For example, averaged over the ten regions, the relative error of the estimates of AWCT mean $\overline{T}_{\text{reg}}$ and standard deviation σ_{reg} for ''standard'' regions (Fig. 1) and for reduced-size regions (by approximately a third of their area) is about 4% and 18%, respectively. Statistical estimates based on different methods of calculating annual means within each region (simple spatial averaging versus distance-weighted averaging) do not differ significantly. The 95% confidence intervals are calculated for peak LFO time periods and are 1.35 σ for the years prior to 1903, 0.40 σ for 1933–48, 0.23 σ for 1963–78, and 0.39 σ for 1993–2002. The 15-yr AWCT means (red horizontal lines in Fig. 2) associated with these multidecadal peak values exceed the confidence intervals and thus are statistically significant.

REFERENCES

Aagaard, K., and E. C. Carmack, 1994: The Arctic Ocean and climate: A perspective. *The Polar Oceans and Their Role in Shaping the Global Environment: The Nansen Centennial Volume, Geophys. Monogr.,* No. 85, Amer. Geophys. Union, 5–20.

——, E. Fahrbach, J. Meincke, and J. H. Swift, 1991: Saline outflow from the Arctic Ocean: Its contribution to the deep waters of the Greenland, Norwegian, and Iceland Seas. *J. Geophys. Res.,* **96,** 20 433–20 441.

Bengtsson, L., V. A. Semenov, and O. M. Johannessen, 2004: The early twentieth-century warming in the Arctic—A possible mechanism. *J. Climate,* **17,** 4045–4057.

Blindheim, J. V. Borovkov, B. Hasen, S. A. Malmberg, W. R. Turrell, and S. Osterhus, 2000: Upper layer cooling and freshening in the Norwegian Sea in relation to atmospheric forcing. *Deep-Sea Res.,* **47A,** 655–680.

Bønisch, G., J. Blindheim, J. L. Bullister, P. Schlosser, and D. W. R. Wallace, 1997: Long-term trends of temperature, salinity, density, and tracers in the central Greenland Sea. *J. Geophys. Res.,* **102,** 18 553–18 571.

Boyd, T. J., M. Steele, R. D. Muench, and J. T. Gunn, 2002: Partial recovery of the Arctic Ocean halocline. *Geophys. Res. Lett.,* **29,** 1657, doi:10.1029/2001GL014047.

Carmack, E. C., R. W. Macdonald, R. G. Perkin, F. A. McLaughlin, and R. J. Pearson, 1995: Evidence for warming of Atlantic water in the southern Canadian Basin of the Arctic Ocean: Results from the Larsen-93 expedition. *Geophys. Res. Lett.,* **22,** 1061–1064.

——, and Coauthors, 1997: Changes in temperature and tracer distributions within the Arctic Ocean: Results from the 1994 Arctic Ocean section. *Deep-Sea Res.,* **44B,** 1487–1502.

Cavalieri, D. J., C. L. Parkinson, and K. Y. Vinnikov, 2003: 30-year satellite record reveals contrasting Arctic and Antarctic decadal sea ice variability. *Geophys. Res. Lett.,* **30,** 1970, doi:10.1029/2003GL018031.

Delworth, T. L., and M. E. Mann, 2000: Observed and simulated multi-decadal variability in the Northern Hemisphere. *Climate Dyn.,* **16,** 661–676.

Dewey, R. K., R. D. Muench, and J. T. Gunn, 1999: Mixing and vertical heat flux estimates in the Arctic Eurasian Basin. *J. Mar. Syst.,* **21,** 199–205.

Dickson, R., J. Lazier, J. Meincke, P. Rhines, and J. Swift, 1996: Long-term coordinated changes in the convective activity of the North Atlantic. *Progress in Oceanography,* Vol. 38, Pergamon, 241–295.

——, and Coauthors, 2000: The Arctic Ocean response to the North Atlantic Oscillation. *J. Climate,* **13,** 2671–2696.

——, I. Yashayaev, J. Meincke, W. R. Turrell, S. Dye, and J. Holfort, 2002: Rapid freshening of the deep North Atlantic Ocean over the past four decades. *Nature,* **416,** 832–837.

Dvorkin, E. N., S. Yu. Kochanov, and N. P. Smirnov, 2000: The North Atlantic Oscillation and long-term changes in the level of the Arctic Ocean. *Russ. Meteor. Hydrol.,* **3,** 59–64.

Enfield, D. B., A. M. Mestas-Nuñez, and P. J. Trimble, 2001: The Atlantic multidecadal oscillation and its relation to rainfall and river flows in the continental U.S. *Geophys. Res. Lett.,* **28,** 2077–2080.

Environmental Working Group, 1997: *Joint U.S.–Russian Atlas of the Arctic Ocean.* National Snow and Ice Data Center, Boulder, CO, CD-ROM.

Gorshkov, S. G., 1980: *Atlas of Oceans. Arctic Ocean* (in Russian). Military Defense Publishing House, 199 pp.

Grotefendt, K., K. Logemann, D. Quadfasel, and S. Ronski, 1998: Is the Arctic Ocean warming? *J. Geophys. Res.,* **103,** 27 679–27 687.

Gudkovich, Z. M., 1961: Relationship between ice drift in the Arctic Basin and ice conditions in the Soviet Arctic seas. *Trans. Oceanogr. Comm.,* **11,** 13–20.

Häkkinen, S., and G. L. Mellor, 1992: Modeling the seasonal variability of a coupled Arctic ice–ocean system. *J. Geophys. Res.,* **97,** 20 285–20 304.

Hurrell, J. W., 1995: Decadal trends in the North Atlantic Oscillation: Regional temperatures and precipitation. *Science,* **269,** 676–679.

——, cited 2003: North Atlantic Oscillation (NAO) indices information. [Available online at http://www.cgd.ucar.edu/~jhurrell/nao.stat.winter.html#winter.]

Johannessen, O. M., M. Miles, and E. Bjorgo, 1995: The Arctic's shrinking sea ice. *Nature,* **376,** 126–127.

Johnson, M. A., A. Y. Proshutinsky, and I. V. Polyakov, 1999: Atmospheric patterns forcing two regimes of Arctic circulation: A return to anticyclonic conditions? *Geophys. Res. Lett.,* **26,** 1621–1624.

Kaplan, A., M. A. Cane, Y. Kushnir, A. C. Clement, M. B. Blumenthal, and B. Rajagopalan, 1998: Analyses of global sea surface temperature 1856–1991. *J. Geophys. Res.,* **103,** 18 567–18 589.

Karcher, M. J., R. Gerdes, F. Kauker, and C. Koberle, 2003: Arctic warming: Evolution and spreading of the 1990s warm event in the Nordic seas and the Arctic Ocean. *J. Geophys. Res.,* **108,** 3034, doi:10.1029/2001JC001265.

Kushnir, Y., 1994: Interdecadal variations in North Atlantic sea surface temperature and associated atmospheric conditions. *J. Climate,* **7,** 141–157.

Lazier, J., 1980: Oceanographic conditions at Ocean Weather Ship Bravo, 1964–1974. *Atmos.–Ocean,* **18,** 227–238.

Martin, S., E. A. Minoz, and R. Drucker, 1997: Recent observations of a spring–summer surface warming over the Arctic Ocean. *Geophys. Res. Lett.,* **24,** 1259–1262.

Maslanik, J. A., M. C. Serreze, and R. G. Barry, 1996: Recent decreases in Arctic summer ice cover and linkages to atmospheric circulation anomalies. *Geophys. Res. Lett.,* **23,** 1677–1680.

McLaughlin, F. A., E. C. Carmack, R. W. Macdonald, and J. K. B. Bishop, 1996: Physical and geochemical properties across the Atlantic/Pacific water mass front in the southern Canadian Basin. *J. Geophys. Res.,* **101,** 1183–1197.

McPhee, M. G., and N. Untersteiner, 1982: Using sea ice to measure vertical heat flux in the ocean. *J. Geophys. Res.,* **87,** 2071–2074.

——, T. P. Stanton, J. H. Morison, and D. G. Martinson, 1998: Freshening of the upper ocean in the Arctic: Is perennial sea ice disappearing? *Geophys. Res. Lett.,* **25,** 1729–1732.

Meincke, J., S. Jonsson, and J. H. Swift, 1992: Variability of convective conditions in the Greenland Sea. *ICES Mar. Sci. Symp.,* **195,** 32–39.

Minobe, S., 1997: A 50–70 year climatic oscillation over the North Pacific and North America. *Geophys. Res. Lett.,* **24,** 683–686.

Morison, J., K. Aagaard, and M. Steele, 1998a: Report on the study of the Arctic Change Workshop. ARCSS Rep. 8, University of Washington, 63 pp.

——, M. Steele, and R. Andersen, 1998b: Hydrography of the upper Arctic Ocean measured from the nuclear submarine U.S.S. *Pargo. Deep-Sea Res.,* **45A,** 15–38.

——, K. Aagaard, and M. Steele, 2000: Recent environmental changes in the Arctic: A review. *Arctic,* **53,** 359–371.

——, and Coauthors, 2002: North Pole Environmental Observatory delivers early results. *Eos, Trans. Amer. Geophys. Union,* **83,** 357, 360–361.

Mysak, L. A., D. K. Manak, and R. F. Marsden, 1990: Sea-ice anomalies observed in the Greenland and Labrador Seas during 1901–1984 and their relation to an interdecadal Arctic climate cycle. *Climate Dyn.,* **5,** 111–133.

Nansen, F., 1902: Oceanography of the North Polar Basin. *Norwegian North Polar Expedition, 1893–1896: Scientific Results,* Vol. 3, No. 9, Kristiania.

Østerhus, S., and T. Gammelsrød, 1999: The abyss of the Nordic seas is warming. *J. Climate,* **12,** 3297–3304.

Overland, J. E., M. C. Spillane, and N. N. Soreide, 2004: Integrated analysis of physical and biological pan-Arctic change. *Climatic Change,* **63,** 291–322.

Pawlowicz, R., and D. Farmer, 1997: Temperature changes in the western Eurasian Basin and northern Fram Strait, 1964–1994. *Eos, Trans. Amer. Geophys. Union,* **76** (3), OS13.

Polyakov, I. V., 1996: Diagnostic calculations of the currents and sea level variations of the Arctic Ocean. *Izv. Atmos. Oceanic Phys.,* **32,** 637–649.

——, and M. A. Johnson, 2000: Arctic decadal and interdecadal variability. *Geophys. Res. Lett.,* **27,** 4097–4100.

——, and Coauthors, 2002: Observationally based assessment of polar amplification of global warming. *Geophys. Res. Lett.,* **29,** 1878, doi:1029/2001GL011111.

——, and Coauthors, 2003a: Variability and trends of air temperature and pressure in the maritime Arctic, 1875–2000. *J. Climate,* **16,** 2067–2077.

——, and Coauthors, 2003b: Long-term ice variability in Arctic marginal seas. *J. Climate,* **16,** 2078–2085.

——, D. Walsh, I. A. Dmitrenko, R. L. Colony, and L. A. Timokhov, 2003c: Arctic Ocean variability derived from historical observations. *Geophys. Res. Lett.,* **30,** 1298, doi:10.1029/2002GL0164412003.

Proshutinsky, A. Yu., and M. A. Johnson, 1997: Two circulation regimes of the wind-driven Arctic Ocean. *J. Geophys. Res.,* **102,** 12 493–12 514.

Quadfasel, D. A., A. Sy, D. Wells, and A. Tunik, 1991: Warming in the Arctic. *Nature,* **350,** 385.

Rigor, I. G., R. L. Colony, and S. Martin, 2000: Variations in surface air temperature observations in the Arctic, 1979–97. *J. Climate,* **13,** 896–914.

Rothrock, D. A., Y. Yu, and G. A. Maykut, 1999: Thinning of the arctic sea-ice cover. *Geophys. Res. Lett.,* **26,** 3469–3472.

Rudels, B., E. P. Jones, L. G. Anderson, and G. Kattner, 1994: On the intermediate depth waters of the Arctic Ocean. *The Polar Oceans and Their Role in Shaping the Global Environment: The Nansen Centennial Volume, Geophys. Monogr.*, No. 85, Amer. Geophys. Union, 33–46.

——, L. G. Anderson, and E. P. Jones, 1996: Formation and evolution of the surface mixed layer and halocline of the Arctic Ocean. *J. Geophys. Res.,* **101,** 8807–8821.

Schauer, U., R. D. Muench, B. Rudels, and L. Timokhov, 1997: Impact of eastern Arctic shelf waters on the Nansen Basin intermediate layers. *J. Geophys. Res.,* **102** (C2), 3371–3382.

Schlesinger, M. E., and N. Ramankutty, 1994: An oscillation in the global climate system of period 65–70 years. *Nature,* **367,** 723–726.

SCICEX, cited 2004: ARCSS Data Catalog. [Available online at http://arcss.colorado.edu/data/arcss.html.]

Serreze, M. C., F. Carse, R. G. Barry, and J. C. Rogers, 1997: Icelandic low cyclone activity: Climatological features, linkages with the NAO, and relationships with recent changes in the Northern Hemisphere circulation. *J. Climate,* **10,** 453–464.

——, and Coauthors, 2000: Observational evidence of recent change in the northern high-latitude environment. *Climatic Change,* **46,** 159–207.

Smethie, W. M., Jr., P. Schlosser, G. Bonisch, and T. S. Hopkins, 2000: Renewal and circulation of intermediate waters in the Canadian Basin observed on the SCICEX 96 cruise. *J. Geophys. Res.,* **105** (C1), 1105–1121.

Steele, M., and T. Boyd, 1998: Retreat of the cold halocline layer in the Arctic Ocean. *J. Geophys. Res.,* **103,** 10 419–10 435.

——, and J. H. Morison, 1993: Hydrography and vertical fluxes of heat and salt northeast of Svalbard in autumn. *J. Geophys. Res.,* **98,** 10 013–10 024.

Swift, J. H., E. P. Jones, K. Aagaard, E. C. Carmack, M. Hingston, R. W. MacDonald, F. A. McLaughlin, and R. G. Perkin, 1997: Waters of the Makarov and Canada basins. *Deep-Sea Res.,* **44,** 1503–1529.

Thompson, D. W. J., and J. M. Wallace, 1998: The Arctic Oscillation signature in the wintertime geopotential height and temperature fields. *Geophys. Res. Lett.,* **25,** 1297–1300.

Treshnikov, A. F., 1985: *Atlas of the Arctic* (in Russian). Main Administration of Geogesy and Cartography, 204 pp.

Tucker, W. B., III, J. W. Weatherly, D. T. Eppler, L. D. Farmer, and D. L. Bentley, 2001: Evidence for rapid thinning of sea ice in the western Arctic Ocean at the end of the 1980s. *Geophys. Res. Lett.,* **28,** 2851–2854.

Venegas, S. A., and L. A. Mysak, 2000: Is there a dominant timescale of natural climate variability in the Arctic? *J. Climate,* **13,** 3412–3434.

Vinje, T., 2001: Anomalies and trends of sea-ice extent and atmospheric circulation in the Nordic seas during the period 1864–1998. *J. Climate,* **14,** 255–267.

Walsh, J. E., W. L. Chapman, and T. L. Shy, 1996: Recent decrease of sea level pressure in the central Arctic. *J. Climate,* **9,** 480–486.

Woodgate, R. A., K. Aagaard, R. D. Muench, J. Gunn, G. Bjork, B. Rudels, A. T. Roach, and U. Schauer, 2001: The Arctic Ocean boundary current along the Eurasian slope and the adjacent Lomonosov Ridge: Water mass properties, transports and transformations from moored instruments. *Deep-Sea Res.*, **148,** 1757–1792.

Yi, D., L. A. Mysak, and S. A. Venegas, 1999: Decadal-to-interdecadal fluctuations of Arctic sea-ice cover and the atmospheric circulation during 1954–1994. *Atmos.–Ocean*, **37,** 389–415.

Zhang, X., J. E. Walsh, J. Zhang, U. S. Bhatt, and M. Ikeda, 2004: Climatology and interannual variability of Arctic cyclone activity, 1948–2002. *J. Climate*, **17,** 2300–2317.